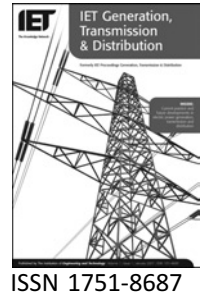


Published in IET Generation, Transmission & Distribution
Received on 20th July 2007
Revised on 21st February 2008
doi: 10.1049/iet-gtd:20070505



Phasor estimation technique to reduce the impact of coupling capacitor voltage transformer transients

E. Pajuelo G. Ramakrishna M.S. Sachdev

*Power System Research Group, Department of Electrical and Computer Engineering, University of Saskatchewan, 57 Campus Drive, Saskatoon, SK, Canada S7N 5A9
E-mail: rama.krishna@usask.ca*

Abstract: A new least squares technique to reduce the impact of the transient response of coupling capacitor voltage transformers (CCVTs) on the performance of distance relays is described. Several factors that affect the frequency and time responses of CCVTs are considered. The effect of the transient response on the phasor-estimates is illustrated. An improved least squares technique, which uses the knowledge of the frequency of the CCVT transients while estimating the phasors, is presented. A case, taken from a set of studies, is included to demonstrate the performance of the proposed approach. The robustness of the method is verified by a CCVT parameter sensitivity study.

1 Introduction

Distance relays are the most widely used devices for protecting transmission lines. These relays need to identify correctly and quickly the presence of a fault to isolate the faulted component with minimum impact to the rest of the network. This seemingly simple requirement is difficult to achieve due to the presence of transient components in the power system voltage and current signals received by the relays.

The coupling capacitor voltage transformer (CCVT) is one important source of the transients measured by distance relays. The CCVT voltage output is accurate only during steady-state conditions, but not so during transients. In this paper, the CCVT transient behaviour is briefly analysed by reviewing the frequency and time domain responses considering the factors that influence them. These responses are obtained using a mathematical model of the CCVT. Existing CCVT models have focused on producing accurate response over a wide frequency range with more emphasis in ferroresonance or switching conditions [1–6]. In this study, the CCVT is modelled from the point of view of protective relaying, that is,

restricting the frequency bandwidth to that typically used by the relay algorithms, and with emphasis on faulted conditions.

Most distance relays use, to make a decision, the fundamental frequency information such as amplitude and angle, which is typically obtained in a digital relay using a phasor estimator. The CCVT transient behaviour causes a delay in the phasor estimator to produce accurate values. The earlier the estimate, the less accurate is the voltage phasor (larger is the phasor error). The protective decision is compromised by this error, which may cause an incorrect operation. To overcome this problem, a method has been suggested that reduces this phasor error based on the study of a particular CCVT [7], but the performance for CCVT and burden parameter variations and different fault scenarios were not demonstrated. Earlier in [8], a method has been proposed that reduces the distortion in the CCVT time response, but the effect on the phasor estimation was not fully evaluated. The authors in [9] and [10] also propose methods to overcome the impact of CCVT transients, but they do not use the CCVT parameters directly.

A new method of estimating the phasors is proposed in this paper. The method is based on the least squares technique and uses the knowledge of the frequencies in the voltage waveforms provided by the CCVTs during transients.

A representative case for a transmission line fault is presented in this paper. The voltages and currents were determined by simulating a power system on the alternative transients program (ATP) software. The results are compared with those obtained by using a least squares technique that does not take into account the transient behaviour of the CCVTs. The results show that there are improvements in terms of speed and accuracy when the proposed method is used.

A study that evaluates the sensitivity of the new method to uncertainty in the knowledge of the CCVT parameters is also presented in this paper. The purpose of the sensitivity study is to understand the order of magnitude of the error introduced by uncertainty in the accuracy of the CCVT parameters. This uncertainty error was compared with the improvements obtained over traditional phasor estimation methods. The results of this study justify the practicality of this method.

2 CCVT characteristics

The CCVTs perform three main functions: scale down the power system voltage to the secondary voltage level required by protection, measurement and control equipments in a substation, provide electrical isolation from the high power system voltage and normalise the secondary voltage to a range typical from 100 to 120 V according to the standards [11] in use.

A CCVT, as shown in Fig. 1, consists of three main elements: capacitive divider, series inductance and intermediate potential transformer (PT). The capacitive divider scales down the high primary voltage to an intermediate level in the range of 5 to

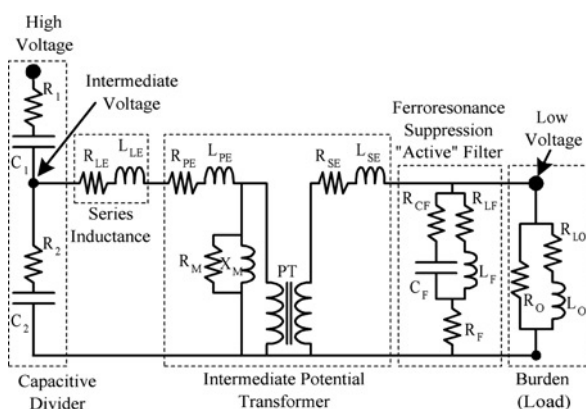


Figure 1 Detailed circuit of a typical CCVT

20 kV. The series inductance compensates the net capacitive reactance of the divider at the power system frequency to minimise the net impedance seen by the intermediate PT. The intermediate PT performs the final voltage reduction to the normalised secondary voltage desired.

The steady-state accuracy of a CCVT is acceptable even for the most demanding applications. The CCVT performance, however, is far from ideal whenever it is subjected to power system voltage transients, such as during fault conditions in the power system. The voltage output signal produced in these conditions contains transient components not present at the CCVT input, that is, the CCVT introduces distortions in the voltage signal [12–14].

2.1 CCVT response

The CCVT behaviour is analysed here by using two kinds of response: frequency response and time response. The frequency response is represented by magnitude and angle responses. A typical CCVT magnitude response is shown in Fig. 2a and has the following characteristics [1–3]: a) gain of 1.0 (pu) at power system fundamental frequency, b) amplification of undesired frequencies, slightly above and slightly below fundamental and c) attenuation of higher frequencies and the DC (0 Hz). As a result, the magnitude (pu) of a fundamental frequency signal is the same at the input and output of a CCVT. This is not the case with a transient signal because it contains several frequencies and each frequency component is amplified or attenuated by the CCVT differently.

A typical CCVT angle response is shown in Fig. 2b and presents the following characteristics: a) angle shift of 0° at fundamental frequency, b) leading angle from DC to fundamental and c) lagging angle for higher frequencies. A fundamental frequency signal is reproduced with the angle unmodified at the CCVT output. Transient signals, however, are affected because each frequency component is shifted in time by the CCVT by a different amount so that the

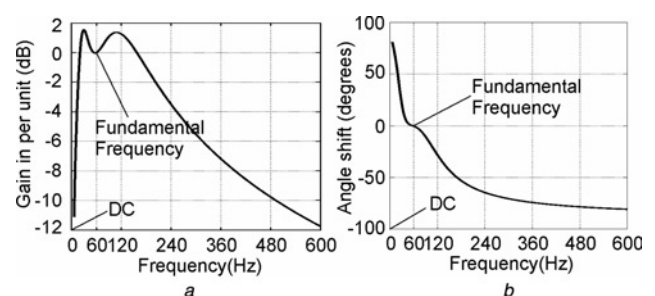


Figure 2 Typical CCVT frequency response

a Magnitude
b Angle

original relative position in time between each of these components is not preserved, that is, the response is not linear with frequency.

There are three main factors that influence the frequency response of a CCVT: the type of the ferroresonance suppression circuit used [2–3], the overall CCVT parameters [1–3, 12, 14], and the characteristics of the burden connected. The burden has negligible effect in the response at the fundamental frequency, because a CCVT is designed to provide good accuracy in steady-state conditions. However, for frequencies outside the fundamental, the behaviour of the burden affects significantly the magnitude and angle response of the CCVT [1, 3, 12, 14].

The time response of a CCVT is very close to an ideal response in steady-state conditions. The transient response, however, includes typically three oscillatory decaying components: a high-frequency decaying component, a low-frequency decaying component and a DC decaying component [13]. A typical CCVT time response is shown in Fig. 3 [15].

The factors that influence the frequency response of a CCVT also affect its time response. Besides, two additional factors affect the time response: the fault incidence angle and the magnitude of voltage change [7, 9, 12, 13].

2.2 CCVT modelling

Fig. 1 shows a detailed representation of a typical CCVT model. The values of its components can be obtained from the CCVT manufacturer, or using measurements as described in [1, 3, 5, 6]. All components used in this representation are considered to be linear during fault conditions in the power system. One of these components typically associated with nonlinear response is the magnetic core of the intermediate PT, represented by the magnetising branch resistance R_M

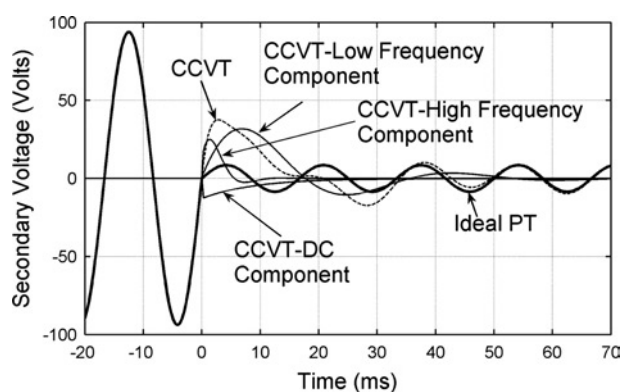


Figure 3 Typical time response of a CCVT showing transient components

and inductance X_M . The nonlinear region is not considered in this study since a fault condition in a power system causes voltage drops [7, 8, 16]. Besides, the possibility of nonlinear ferroresonance is minimised by the appropriate suppression circuit. The only condition where ferroresonance was observed in the course of this study is immediately after removing a short circuit on the secondary of the CCVT. This condition is an internal CCVT fault and therefore it was not considered in this study. Other components associated with nonlinear response are the overvoltage protecting air gaps that spark temporarily during conditions of fast transient overvoltage or internal failure of the CCVT. These gaps are not considered because they should not operate for the power system fault conditions considered in this study.

Stray capacitances, typically present in coil winding constructions such as inductances or power transformers, are also neglected in this model representation. These capacitances influence the response only at high frequencies, in the order of 1–2 kHz [1–3], far from the bandwidth of the filtering performed in this study.

Two methods were used to construct the mathematical model of the CCVT: Laplace and ATP/EMTP. Using Laplace, a transfer function was obtained that provided desired characterising parameters such as natural frequencies and decaying time constants. To simplify this transfer function, R_M and X_M can be neglected, because in the linear region their effect is very small. Another simplification that was used here is the removal of paired zeros and poles of the same value far from the imaginary axis. Another point worth mentioning is that the parameters C_2 , L_{LE} , R_F , C_F and L_F are the ones that most affect the location of the poles of this transfer function. For the CCVT used, a fifth-order transfer function was obtained as shown in (1). The details of how to arrive at (1) are provided in Appendix 2. The ATP/EMTP [17] method was used to simulate the power system fault conditions including the CCVT response. In this last method, no simplifications are needed, and even the nonlinearity could be included.

$$G(s) = \frac{K_{CCVT}(s - z_1)(s - z_1^*)(s - z_2)(s - z_3)}{(s - p_1)(s - p_1^*)(s - p_2)(s - p_2^*)(s - p_3)} \quad (1)$$

where

$$p_1 = \sigma_1 + j \cdot \omega_1; \quad \text{high-frequency poles}$$

$$p_2 = \sigma_2 + j \cdot \omega_2; \quad \text{low-frequency poles}$$

$$p_3 = \sigma_3; \quad \text{dc pole}$$

3 Impact of CCVT transients on distance protection

3.1 Basic concepts

A basic distance relay measures the voltage at the relay location and the current flowing in the protected line. A signal-processing technique is used to convert the sampled values of a voltage to fundamental frequency phasor V_R , and the sampled values of a current to fundamental frequency phasor I_R . From these phasors, the relay compares $I_R Z_L$ (Z_L being the reach of the relay) with V_R to decide if the present power system condition is a fault and whether it is inside the zone protected by the relay. Notice that $I_R Z_L$ and V_R are equal for a zero ohm fault ($R_F = 0$) at the reach of the relay, as shown in Fig. 4. The errors in the estimates of the magnitude and angle of the phasor affect the operation of the distance function in many situations. These errors cause undesired overreach or underreach, also shown in Fig. 4. Besides, the speed in obtaining accurate phasors is one factor that determines the operating speed of the relay.

3.2 Impact of CCVT transients

In digital distance relays, the transient components introduced by the CCVT affect negatively the accuracy and cause delay in the phasor estimation process, that is, they produce a temporary phasor error. This phasor error caused by the CCVT presents some typical characteristics: a) duration limited in time in the range of three to five cycles, b) amount dependent on the CCVT response characteristics, c) behaviour decaying and oscillating in time. Obviously, the phasor error also depends on the quality of the estimation method used. To illustrate this behaviour, in Fig. 5 the phasors are obtained from the signals CCVT and Ideal PT of Fig. 3.

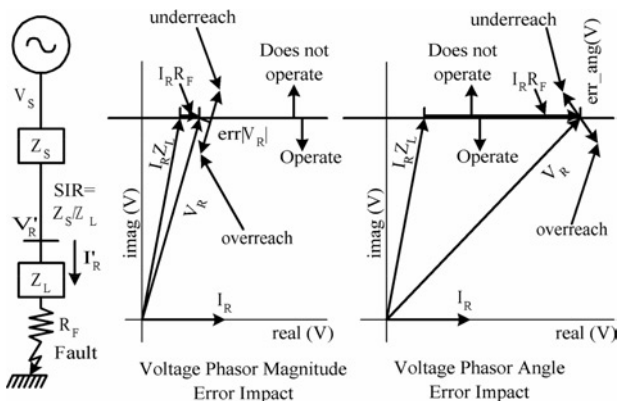


Figure 4 Impact of voltage phasor estimation errors in the distance protection

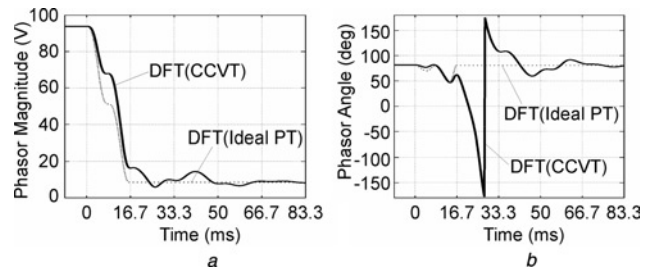


Figure 5 Comparison of estimated phasors showing a Magnitude error b Angle error

The phasor error affects the performance of distance protection by producing transient overreach and/or underreach. The problem becomes worse in systems with larger source to line impedance ratio (SIR) conditions. The voltage at the relay location during a fault is a function of the SIR. A higher SIR translates into a larger voltage change at the relay location on the inception of a fault, because the voltage at the relay location is lower compared with the voltage experienced if the SIR were smaller.

To illustrate these phenomena, a fault at the remote end of a line was considered and performances of CCVT and distance functions with and without the transients were evaluated. For comparison, the quality of phasor estimates was considered. The voltage phasor was estimated using the DFT technique [18] that uses a one cycle data window. The DFT technique is commonly used in the relaying functions and is equivalent to the basic least squares method that is described in Section 4 [19]. The impact of the transients in the current was eliminated by using the steady-state phasor of the fault current.

Fig. 6a shows the phasors for a system with an SIR of 10, which typically indicates that either the power

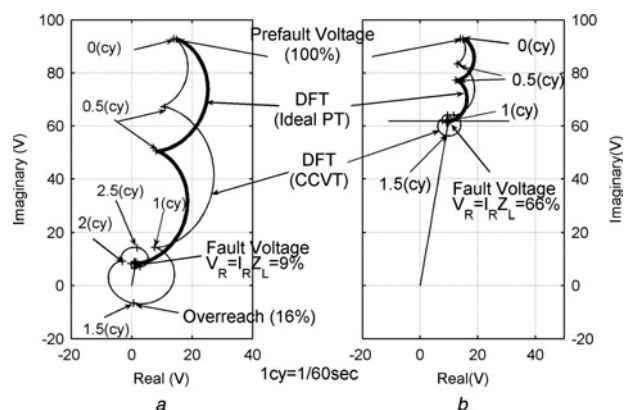


Figure 6 Estimated voltage phasor overreach comparison of CCVT and ideal PT

a SIR = 10
b SIR = 0.5

system source is weak or that the protected line is short. The transient overreach is larger than the voltage drop in the line impedance Z_L , that is the error in distance computation is larger than 100%. The risk of false operation of the protection function is therefore very high unless appropriate countermeasures are taken. On the other hand, the response for an ideal PT converges to the correct value after one cycle, which is the nominal delay of the full cycle DFT technique.

A smaller SIR typically corresponds to a stronger power system source. This case is illustrated in Fig. 6b; for an SIR of 0.5 the overreach is very small compared with the high SIR case of Fig. 6a.

The operating time of the distance function can be shorter than the convergence time of the phasor estimator, under low SIR conditions. However, for high SIR conditions, the distance operating time has to wait for the convergence of the phasor estimator. In Fig. 6b, an operating time of one cycle is acceptable for most faults, whereas in Fig. 6a more than three cycles are needed. In this paper a new method to improve the response for high SIR such as the case of Fig. 6a is described in Section 4.3.

3.3 Techniques for minimising the impact of CCVT transients

In general, the techniques to overcome the CCVT problem can be classified in three main groups: 1) avoid using the voltage phasor during CCVT transients, 2) wait for the transient to subside and 3) use intelligently the phasors obtained during this transient interval. An example for the first group is the memory voltage technique [16, 20, 21]. In this technique, the voltage measured is memorised before a transient starts, then during the transient interval this memorised phasor is used instead of the distorted value. In the second group, a time delay is introduced before a decision is made [9, 16]. For instance, a time delay of five cycles would be needed if an accurate measurement is required. A fixed delay is not always compatible with the power system critical clearing times, in the order of 100 ms, that is, the maximum time a fault can be withstood without compromising the stability of the network. Adaptive time delay schemes are useful in this case.

The third group can be subdivided in other three categories: 1) compensate for the error, 2) identify and reduce the error and 3) use of additional power system characteristics. In the first category, the maximum deviation caused by a CCVT transient is estimated upfront. This deviation is then plotted in the complex plane as an uncertainty region around the undistorted operating point. Knowing this region, the

protective function is adjusted so as not to enclose any incorrect operating point [7, 9, 10]. In the second category, special filters have been proposed that are applied before the phasor estimator [7, 8]. The response time of this last approach in obtaining a phasor is the sum of the delay introduced by the filter and the inherent phasor estimator delay. In the third category, the use of additional power system characteristics has been a traditional approach in the relaying industry [9, 20]. The new method proposed in this paper falls under the second category of this group and is described in Section 4.

4 Extended least squares technique

4.1 Basic least squares approach

This algorithm is based on fitting a specified waveform to a set of measurements as shown in Fig. 7. The best fitting is obtained by minimising the sum of squares of the differences between the measurements and the waveform. For achieving this objective, the mathematical description of the waveform must be selected upfront [19].

The waveform is assumed to be a time dependent sine function of known frequency, ω_0 , but of an unknown magnitude and phase angle. This waveform is decomposed into two orthogonal sine and cosine functions of unknown amplitudes V_R and V_I . The difference from the observed signal, say voltage v , and the proposed waveform is assumed to be noise ε .

An over-defined set of linear equations is established based on the measured samples of the voltage v , the time dependent sine and cosine coefficients and the unknown parameters V_R and V_I . The coefficients are functions of time $t - t_0$ ($=k\Delta t$, $k = 1, \dots, N$), where Δt is the sampling period. The number of measured samples, N , used in estimating the phasor is also called the data window size, which is sometimes expressed in cycles of the nominal frequency. The set of linear equations

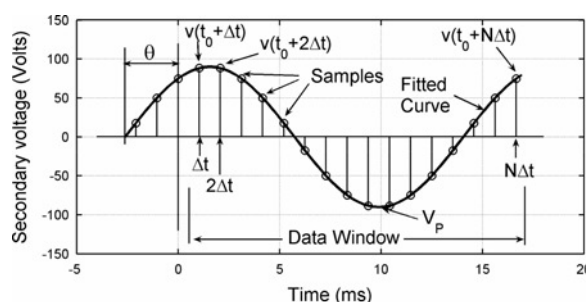


Figure 7 Basic least squares curve fitting for phasor estimation

can be written as

$$\begin{bmatrix} \sin(\omega_0 \Delta t) & \cos(\omega_0 \Delta t) \\ \sin(\omega_0 2\Delta t) & \cos(\omega_0 2\Delta t) \\ \vdots & \vdots \\ \sin(\omega_0 N\Delta t) & \cos(\omega_0 N\Delta t) \end{bmatrix} \begin{bmatrix} V_R \\ V_I \end{bmatrix} = \begin{bmatrix} v(t_0 + \Delta t) \\ v(t_0 + 2\Delta t) \\ \vdots \\ v(t_0 + N\Delta t) \end{bmatrix} \quad (2)$$

In the matrix notation, this is

$$[A][x] = [b] \quad (3)$$

The vector of unknowns is determined by using the left pseudo-inverse of $[A]$ as follows

$$[x] = [[A]^T[A]]^{-1}[A]^T[b] \quad (4)$$

One of the important advantages of this non-recursive least squares algorithm is that the pre-filtering and phasor estimation are done in one step.

4.2 Limitations of the basic least squares approach

The basic least squares (LSQ-basic) approach has difficulty estimating the fundamental frequency phasor for a voltage signal containing CCVT transient components. This is illustrated in Fig. 8 in which the waveform of the phasor obtained using the basic least squares approach is shown. This waveform is substantially different from the one that would have provided correct phasor magnitude and angle (i.e. ideal PT).

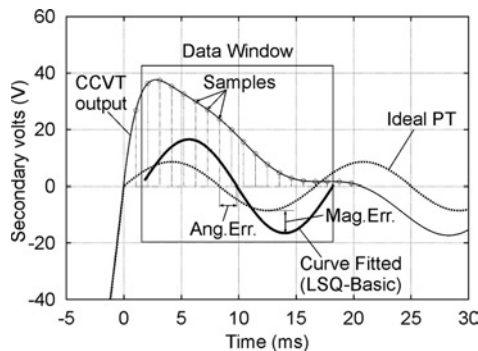


Figure 8 Problem of basic least squares in CCVT applications

4.3 Extended least squares technique

The quality of the phasor estimated depends on the effectiveness of the curve fitting process. To overcome the problem that exists with the basic least squares method, the information concerning the CCVT transfer function and burden can be included in the phasor estimating algorithm if it is available. Considering the example described in Section 2.1, the model of the CCVT output can be expressed as a sum of the waveform of the fundamental frequency ω_0 , a few oscillatory decaying components and a decaying DC component. Including the frequencies ω_1 and ω_2 , time constants of their decays, σ_1 and σ_2 , and the DC component with time constant σ_3 , in the waveform provides the following equation.

$$v = V_R \sin(\omega_0 t) + V_R \cos(\omega_0 t) + V_{R1} e^{(\sigma_1)t} \sin(\omega_1 t) + V_{I1} e^{(\sigma_1)t} \cos(\omega_1 t) + V_{R2} e^{(\sigma_2)t} \sin(\omega_2 t) + V_{I2} e^{(\sigma_2)t} \cos(\omega_2 t) + V_3 e^{(\sigma_3)t} + \varepsilon \quad (5)$$

The frequencies ω_1 and ω_2 for the CCVT used in this study are 0.47 and 1.38 of the fundamental.

The matrix A is now defined by

$$[A] = \begin{bmatrix} A_0 & A_1 & A_2 & A_3 \\ N \times 7 & N \times 2 & N \times 2 & N \times 1 \end{bmatrix} \quad (6)$$

In this equation, $[A_0]$ is identical to the basic least squares matrix $[A]$ on (3), and the others are defined by (7) to (9). The vector of the unknown is defined by (10). Once the matrices are defined, finding the unknown requires the calculation of the left pseudo-inverse using (4).

$$[A_1] = \begin{bmatrix} e^{\Delta t \cdot \sigma_1} \sin(\omega_1 \Delta t) & e^{\Delta t \cdot \sigma_1} \cos(\omega_1 \Delta t) \\ e^{2\Delta t \cdot \sigma_1} \sin(\omega_1 2\Delta t) & e^{2\Delta t \cdot \sigma_1} \cos(\omega_1 2\Delta t) \\ \vdots & \vdots \\ e^{N\Delta t \cdot \sigma_1} \sin(\omega_1 N\Delta t) & e^{N\Delta t \cdot \sigma_1} \cos(\omega_1 N\Delta t) \end{bmatrix} \quad (7)$$

$$[A_2] = \begin{bmatrix} e^{\Delta t \cdot \sigma_2} \sin(\omega_2 \Delta t) & e^{\Delta t \cdot \sigma_2} \cos(\omega_2 \Delta t) \\ e^{2\Delta t \cdot \sigma_2} \sin(\omega_2 2\Delta t) & e^{2\Delta t \cdot \sigma_2} \cos(\omega_2 2\Delta t) \\ \vdots & \vdots \\ e^{N\Delta t \cdot \sigma_2} \sin(\omega_2 N\Delta t) & e^{N\Delta t \cdot \sigma_2} \cos(\omega_2 N\Delta t) \end{bmatrix} \quad (8)$$

$$[A_3] = \begin{bmatrix} e^{\Delta t \cdot \sigma^3} \\ e^{2\Delta t \cdot \sigma^3} \\ \vdots \\ e^{N\Delta t \cdot \sigma^3} \end{bmatrix} \quad (9)$$

$$[x] = [V_R \quad V_I \quad V_{R1} \quad V_{I1} \quad V_{R2} \quad V_{I2} \quad V_3]^T \quad (10)$$

From (10), only the two unknowns V_R and V_I corresponding to the fundamental frequency component are desired, therefore only the first two rows of the pseudo-inverse need to be used, that is the real and the imaginary components.

The phasor estimation process is repeated every time a new sample is available, adding the new sample to the set of N elements and discarding the oldest one. The coefficient matrix needs to be calculated before the first set of N samples is processed, and then remains unmodified. Therefore the left pseudo-inverse only needs to be calculated once. Two parameters need to be defined before the coefficient matrix is constructed: the number N of samples and the sampling period Δt , i.e. the time window $N\Delta t$.

4.4 Selection of time window

The time window represents an inherent delay in the phasor estimation process, because this window should be completely inside the fault to produce a reliable estimate. Then, a shorter time window is desired to obtain a fast protective operation, that is, more speed. However, a longer time window should result in a more accurate estimate, because more data is used. Therefore the optimum time window should be a careful balance between speed and accuracy.

The time window is defined by $N\Delta t$. The sampling period Δt is selected to obtain a reasonable frequency bandwidth that represents the signal being processed. A value of 3840 Hz (=64 samples/cycle in 60 Hz

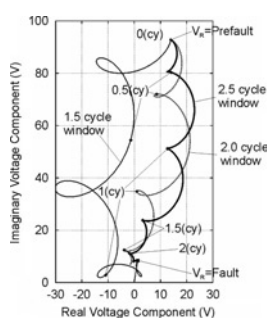


Figure 9 Plot of phasor trajectory of prefault to fault transition

power systems) is representative of the state of the art in protective relaying and was used in this study. The whole problem then becomes the finding of the number of samples N .

The response of the phasor estimator with different values of N is then evaluated using two criteria. One of the criterias is the plot of the voltage phasor trajectory in the complex plane of the transition from prefault to fault, as shown in Fig. 9. The uncertainty in the trajectory is observed and compared. The other criterion is the frequency response of the estimator. The responses of real and imaginary estimators are plotted; this is shown in Fig. 10. The gain or attenuation for frequencies outside the desired fundamental is observed and compared.

Data window sizes N of 64, 96, 128 and 160 samples were considered in this study. The response showed significant improvements up to a value of $N = 128$ (=2 cycles). For higher values of N the results did not show major improvements. Lower values of N showed undesired behaviour. For these reasons, the value of $N = 128$ corresponding to a two cycle window size was selected as the optimum data window size.

4.5 Simulation and results

The technique was tested by performing fault simulations on a realistic power system network configuration using the ATP/EMTP software. An example is presented in this section. In this example, a 500 kV line is 400 km long and the SIR is 6.2 in the weaker end. The fault location is the remote end of the line and the fault incident angle is 0° . The sampling rate used in this example was 3840 Hz.

Fig. 11 shows the voltages provided by an ideal PT and the modelled CCVT. The phasors calculated with the proposed algorithms using a two cycle time window are shown in Figs. 12 and 13.

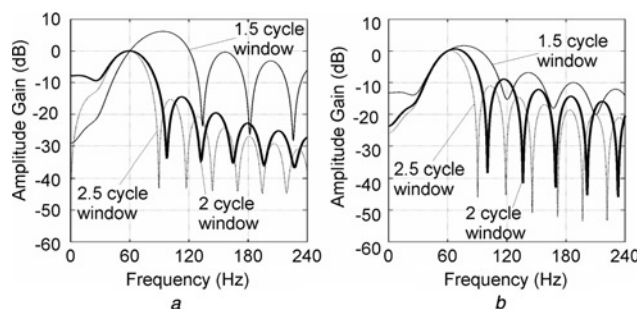


Figure 10 Frequency response of estimator

a Real component
b Imaginary component

The magnitude and angle of the phasors show that they are within a reasonable margin to decide the operation of the relay two cycles after the inception of the fault. Compared with this, the phasors calculated by using the basic least squares technique stabilise four cycles after the inception of the fault.

5 Algorithm sensitivity analysis

5.1 Introduction

The results previously presented assume that the parameters of the CCVT are known with good accuracy. In a real scenario these parameters are known, but with some percentage of errors. To evaluate the impact of these errors on the response of the proposed algorithm, a parameter sensitivity study was performed.

5.2 Definition of the reference condition

A reference condition is defined to compare the effect of CCVT parameter variations on the response of the proposed algorithm. The parameters used to model the CCVT and the burden are used to produce the required linear transfer function. From this function, the characteristic frequencies and time constants are obtained and are used to build the improved least squares algorithm. This is considered to be the ideal case in which the parameters are known with good accuracy.

For this reference condition a fault was simulated where the effect of the error introduced by the CCVT is more noticeable. This same fault was used for all parameter variations. A system with an SIR = 30 was selected, which resulted in a significant change on the voltage magnitude. A fault incidence angle of zero was considered. A very low fault resistance, $R_F = 0.01 \Omega$ was selected. The fault was considered at the remote end of the line. This location is used typically to evaluate transient overreach and underreach in distance protection applications.

The voltage waveform received from the CCVT was processed by the extended least squares algorithm. The magnitude and angle of the voltage phasor provided by

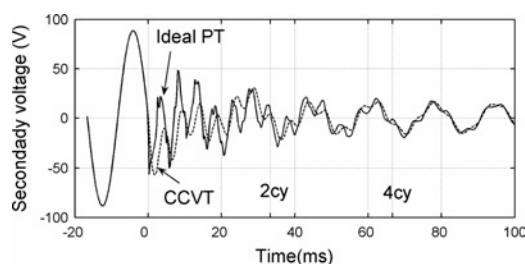


Figure 11 Voltages provided by an ideal PT and the CCVT

the algorithm were used as the reference for determining the impact of parameter variations. The extended least squares algorithm converges to stable phasor values two cycles after the inception of the fault. This is because here a very simple power system was chosen and therefore the deviations were caused exclusively by the parameter variations.

5.3 Parameter variations

Two kinds of parameter variations were studied, single and combined. In the single variation, one of the CCVT parameters was modified by $\pm 5\%$. The reference fault condition was then simulated using the modified CCVT to scale down the primary voltage. The corresponding voltage samples were processed using the improved least squares algorithm that was based on the original CCVT parameters. In the combined variation, several parameters were modified simultaneously, all of them by the same percentage and sign.

The effect of the burden was also considered by including a combined variation of 5%. It is not expected that the burden may be known with less accuracy than that.

Also, two kinds of deviations were measured, steady state and transient. The steady-state deviation was considered to be the difference of the pre-fault voltage magnitude and angle compared with the reference condition. This steady-state deviation represents the impact of the specific parameter on the accuracy of the CCVT. The transient deviation was considered to be the maximum absolute difference in the magnitude and angle compared with the corresponding final stable value. The first two cycles after the inception of the fault were ignored for determining the transient deviation because the improved least squares window was not full of the fault data. This transient deviation is a measure of the uncertainty in the estimation of

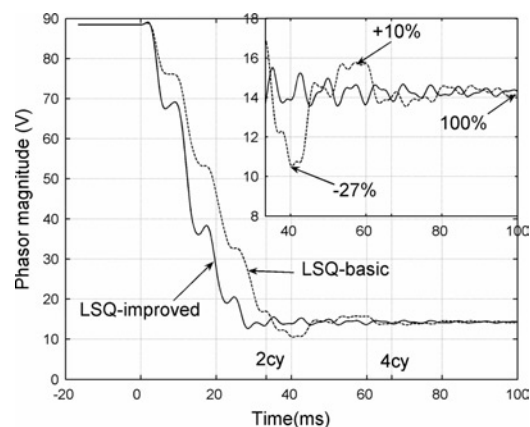


Figure 12 Estimated magnitudes of the phasors

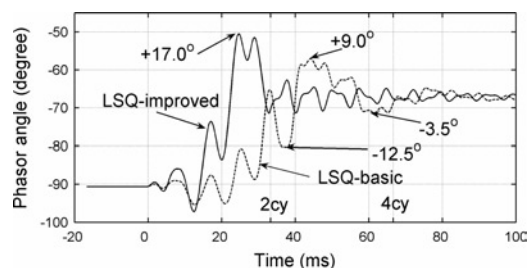


Figure 13 Estimated angles of the phasors

the fault voltage introduced by the variations of the parameters.

5.4 Observations

The results of the parameter sensitivity study are summarised in Tables 1 and 2. The steady-state deviation shows the direct impact on the accuracy of the CCVT that the capacitors C_1 and C_2 have, when they are varied individually. A practical CCVT design would not compromise the overall accuracy by allowing a large uncertainty in the capacitor divider parameters; therefore these two particular variations are disregarded. The combined variation of these capacitors is the next one in the order of significance, without affecting the accuracy too much. Another parameter that significantly affects this steady-state deviation is the series inductance L_{LE} .

In reality, the CCVT parameters do not vary arbitrarily in the way that has been shown here. It is the parameter uncertainty and the robustness of the

Table 1 Steady-state deviation in pre-fault voltage phasor measurement for a 5% increase in the parameter(s)

CCVT parameter	Magnitude deviation, %	Angle deviation, °
C_1	+ 5.	-0.015
C_2	-5.	-0.511
R_{LE}	- 0.030	+0.007
L_{LE}	-0.310	-0.489
R_{PE}	- 0.030	+0.006
L_{PE}	- 0.020	-0.032
R_{SE}	-0.050	+0.010
L_{SE}	-0.020	-0.027
R_F	-0.004	+0.003
C_F	- 0.068	-0.079
L_F	- 0.027	-0.063
C_1, C_2	- 0.340	-0.525

Table 2 Absolute transient deviation in fault voltage after two cycles for an absolute variation of 5% in the parameter(s)

CCVT parameter	Magnitude deviation, %	Angle deviation, °
C_1	0.012	0.14
C_2	0.545	7.35
R_{LE}	0.004	0.10
L_{LE}	0.105	1.38
R_{PE}	0.007	0.10
L_{PE}	0.009	0.13
R_{SE}	0.006	0.14
L_{SE}	0.008	0.12
R_F	0.120	1.58
R_{CF}	0.005	0.05
C_F	0.107	2.78
R_{LF}	0.020	0.48
L_F	0.242	2.81
C_1, C_2	0.555	7.49
R_O, R_{LO}, L_O	0.176	3.20

proposed method to these uncertainties what is being simulated in these parameter variation studies.

The results of the transient deviation, shown in Table 2, are of significant importance. These results indicate that the uncertainty in the phasor estimation is what causes the transient overreach or underreach. The maximum transient error is observed for a combined variation of C_1 and C_2 of 5%. The percentages in the transient magnitude deviation in

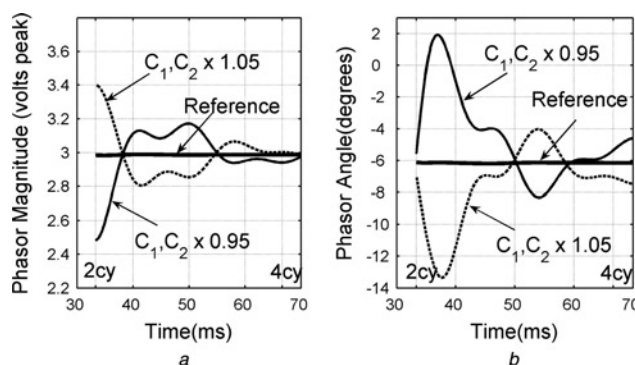


Figure 14 Transient magnitude deviation for a combined variation of C_1 and C_2

a Magnitude
b Angle

Table 2 are taken relative to the corresponding prefault voltage. This maximum transient error is illustrated in Fig. 14. For this case, the basic least squares method produced a deviation of 3 V in magnitude and 180° in angle.

The combined variation of C_1 and C_2 was considered, because they are the ones with most noticeable deviation. The combined variation of R_0 , R_{L0} and L_0 was considered to include the uncertainty in measuring the burden parameters.

6 Conclusions

This paper described the impact of CCVT transients on estimating the phasors of voltages for use in numerical relays. The traditional techniques that do not correctly estimate the phasors during the first few cycles after the inception of a fault are likely to cause the distance and other relays to operate incorrectly.

The knowledge of the CCVT design and the connected burden is incorporated in the relay algorithm. This improved the correctness of the calculated phasors. A least squares technique that included this knowledge was described and demonstrated in this paper. The results show significant improvements in both accuracy and speed.

The accuracy with which the CCVT parameters are known does affect the performance of the proposed algorithm. However, the sensitivity study shows that for a reasonable level of parameter uncertainty the new algorithm performed well.

7 Acknowledgment

A part of this work was published in the Canadian Conference of Electrical and Computer Engineering (CCECE), Conference Proceedings, Saskatoon, Canada, May 2005, pp. 454–457.

8 References

- [1] IRAVANI M.R., WANG X., POLISHCHUK I., RIBEIRO J., SHARSHAR A.: 'Digital time-domain investigation of transient behaviour of coupling capacitor voltage transformer', *IEEE Trans. Power Deliv.*, 1998, **13**, (2), pp. 622–629
- [2] TZIOUVARAS D.A., MCLAREN P., ALEXANDER G., ET AL.: 'Mathematical models for current, voltage, and coupling capacitor voltage transformers', *IEEE Trans. Power Deliv.*, 2000, **15**, (1), pp. 62–72
- [3] KEZUNOVIC M., FROMEN C.W., NILSSON S.L.: 'Digital models of coupling capacitor voltage transformers for protective relay transient studies', *IEEE Trans. Power Deliv.*, 1992, **7**, (4), pp. 1927–1935
- [4] LUCAS J.R., MCLAREN P.G., KEERTHIPALA W.W.L., JAYASINGHE R.P.: 'Improved simulation models for current and voltage transformers in relay studies', *IEEE Trans. Power Deliv.*, 1992, **7**, (1), pp. 152–159
- [5] VERMEULEN H.J., DANN L.R., VAN ROOIJEN J.: 'Equivalent circuit modelling of a capacitive voltage transformer for power system harmonic frequencies', *IEEE Trans. Power Deliv.*, 1995, **10**, (4), pp. 1743–1749
- [6] FERNANDES D., NEVES W.L.A., VASCONCELOS J.C.A., GODOY M.V.: 'Capacitor voltage transformer: laboratory tests and digital simulations'. IPST Conf., Montreal, Canada, June 2005
- [7] KASZTENNY B., SHARPLES D., ASARO V., POZZUOLI M.: 'Distance relays and capacitive voltage transformers – balancing speed and transient overreach' (General Electric Company, GER-3986, 2000)
- [8] IZYKOWSKI J., KASZTENNY B., ROSOLOWSKI E., SAHA M.M., HILLSTROM B.: 'Dynamic compensation of capacitive voltage transformers', *IEEE Trans. Power Deliv.*, 1998, **13**, (1), pp. 116–122
- [9] HOU D., ROBERTS J.: 'Capacitive voltage transformer: transient overreach concerns and solutions for distance relaying'. Canadian Conf. Electrical and Computer Engineering, Calgary, Canada, May 1996, vol. 1, pp. 119–125
- [10] ADAMIAK M.G., ALEXANDER G.E., PREMERLANI W.: 'Advancements in adaptive algorithms for secure high speed distance protection' (General Electric Company, GER-3962, 1996)
- [11] IEC 60044-5: 'International standard – instrument transformers – Part 5: capacitor voltage transformers', 2004
- [12] SWEETANA A.: 'Transient response characteristics of capacitive potential devices', *IEEE Trans. Power Appar. Syst.*, 1971, **PAS-90**, (5), pp. 1989–2001
- [13] BERDY J., BROOKES R., CHADWICK J.W., ET AL.: 'Transient response of coupling capacitor voltage transformers IEEE committee report', *IEEE Trans. Power Appar. Syst.*, 1981, **PAS-100**, (12), pp. 4811–4814
- [14] GERTSCH G.A., ANTOLIC F., GYGAX F.: 'Capacitor voltage transformers and protective relays', CIGRE Report 31–14, 1968
- [15] PAJUELO E., RAMAKRISHNA G., SACHDEV M.S.: 'An improved voltage phasor estimation technique to minimize the

impact of CCVT transients in distance protection'. CCECE 2005, Canadian Conf. Electrical and Computer Engineering, Conf. Proc., Saskatoon, Canada, May 2005, pp. 454–457

[16] HUGHES M.A.: 'Distance relay performance as affected by capacitor voltage transformers', *IEE Proc.*, 1974, **121**, (12), pp. 1557–1566

[17] CANADIAN/AMERICAN EMTP USER GROUP : 'Alternative transients program rule book' (Canadian/American EMTP User Group, 1999)

[18] PHADKE A.G., THORP J.S.: 'Computer relaying for power systems' (Research Studies Press Ltd., Taunton, Somerset, UK, 1988)

[19] SACHDEV M.S., BARIBEAU M.A.: 'A new algorithm for digital impedance relays', *IEEE Trans. Power Appar. Syst.*, 1979, **PAS-98**, (6), pp. 2232–2240

[20] ALEXANDER G.E., ANDRICHAK J.G., TYSKA W.Z.: 'Relaying short lines', in 'GE power management' (General Electric Company, GER-3735, 1992)

[21] ELMORE W.A.: 'Protective relaying theory and applications' (Marcel Dekker Inc., 2004, 2nd edn.)

9 Appendix 1: assumed CCVT parameters

Capacitor Divider:

$$R_1 = 3310.7 \Omega$$

$$C_1 = 0.001605 \times 10^{-6} \text{ Farad}$$

$$R_2 = 59.0338 \Omega$$

$$C_2 = 0.089991 \times 10^{-6} \text{ Farad}$$

Inductance

$$R_{LE} = 950.06 \Omega$$

$$L_{LE} = 67922 \times 10^{-3} \text{ Henry}$$

Internal PT

$$R_{PE} = 850.02 \Omega \text{ – primary side}$$

$$L_{PE} = 4443.3 \times 10^{-3} \text{ Henry}$$

$$R_{SE} = 0.2467 \Omega \text{ – secondary side}$$

$$L_{SE} = 0.64991 \times 10^{-3} \text{ Henry}$$

$$NT = 75.8503 = 5058/66.7 \text{ V}$$

Ferroresonant suppression circuit

$$R_F = 13.333 \Omega$$

$$R_{CF} = 0.08 \Omega$$

$$C_F = 165.36 \times 10^{-6} \text{ Farad}$$

$$R_{LF} = 1.2301 \Omega$$

$$L_F = 54.3 \times 10^{-3} \text{ Henry}$$

Burden

$$R_O = 29.551 \Omega \text{ s}$$

$$R_{LO} = 0 \Omega \text{ s}$$

$$L_O = 0.0982 \text{ Henry s}$$

10 Appendix 2: CCVT transfer function modeling

The simplified circuit that was used in this development is shown in Fig. 15.

In Fig. 15, z_{C1} , z_{C2} is the capacitive divider z_L includes series inductance and resistance, primary and secondary leakage inductance and resistance, z_F is the ferroresonance suppression circuit and z_B is the burden

The input voltage, V_I , and the capacitive divider were simplified using the Thevenin Theorem. From this circuit, the output voltage V_O can be expressed as a function of the input voltage V_I , using the voltage

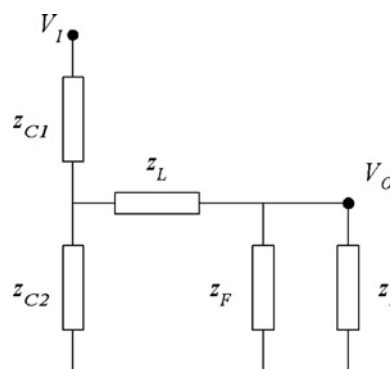


Figure 15 CCVT simplified model

divider technique, thus obtaining

$$V_O = \frac{V_I z_{C2}}{z_{C1} + z_{C2}} \frac{(z_F z_B / (z_F + z_B))}{(z_{C1} z_{C2} / (z_{C1} + z_{C2})) + z_L + (z_F z_B / (z_F + z_B))} \quad (11)$$

$$\frac{V_O}{V_I} = \frac{z_{C2}}{z_{C1} + z_{C2}} \frac{z_F z_B}{((z_{C1} z_{C2} / C_1 + z_{C2})) + z_L (z_F + z_B) + z_F z_B} \quad (12)$$

A change of variables is used to simplify (12)

$$\frac{r}{s} = z_F \quad (13)$$

$$\frac{t}{u} = z_B \quad (14)$$

$$\frac{v}{w} = \frac{z_{C1} z_{C2}}{z_{C1} + z_{C2}} \quad (15)$$

$$\frac{x}{y} = \frac{z_{C2}}{z_{C1} + z_{C2}} \quad (16)$$

Substituting (13)–(16) into (12) gives

$$\frac{V_O}{V_I} = \frac{x}{y} \frac{(r/s)(t/u)}{y[(v/w) + z_L][(r/s) + (t/u)] + (r/s)(t/u)} \quad (17)$$

Simplifying the right-hand side of this equation gives

$$\frac{V_O}{V_I} = \frac{xrtw}{y[vru + vst + z_L wru + z_L wst + wrt]} \quad (18)$$

For this method to be effective, each individual variable is arranged to be a polynomial of the Laplace variable, s . The polynomials are obtained from the

detailed model of Fig. 1, as follows

$$\frac{r}{s} = \frac{R_F + (R_{CF} + (1/sC_F))(R_{LF} + sL_F)}{R_{CF} + (1/sC_F) + R_{LF} + sL_F} \quad (19)$$

$$\frac{r}{s} = \frac{s^2 C_F L_F (R_{CF} + R_F) + s[C_F (R_F R_{CF} + R_F R_{LF} + R_{CF} R_{LF}) + L_F] + (R_F + R_{LF})}{s^2 C_F L_F + s C_F (R_{CF} + R_{LF}) + 1} \quad (20)$$

$$\frac{t}{u} = \frac{(R_O)(R_{LO} + sL_O)}{R_O + R_{LO} + sL_O} = \frac{sR_O L_O + R_O R_{LO}}{sL_O + (R_O + R_{LO})} \quad (21)$$

$$\begin{aligned} \frac{v}{w} &= \frac{(R_1 + (1/sC_1))(R_2 + (1/sC_2))}{R_1 + (1/sC_1) + R_2 + (1/sC_2)} \\ &= \frac{s^2 R_1 R_2 C_1 C_2 + s(R_1 C_1 + R_2 C_2) + 1}{s^2 C_1 C_2 (R_1 + R_2) + s(C_1 + C_2)} \end{aligned} \quad (22)$$

$$\begin{aligned} \frac{x}{y} &= \frac{(R_2 + (1/sC_2))}{R_1 + (1/sC_1) + R_2 + (1/sC_2)} \\ &= \frac{sR_2 C_2 + 1}{sC_2 (R_1 + R_2) + (1 + (C_2/C_1))} \end{aligned} \quad (23)$$

$$z_L = R_{LE} + sL_{LE} + R_{PE} + sL_{PE} + R_{SE} + sL_{SE} \quad (24)$$

$$z_L = s(L_{LE} + L_{PE} + L_{SE}) + (R_{LE} + R_{PE} + R_{SE}) \quad (25)$$

To obtain the overall transfer function, the variables in (19)–(25) are substituted, in the numerator and denominator of (18), by the corresponding polynomials in ‘ s ’ that use the values of the appropriate CCVT parameters. A fifth-order transfer function is obtained for a typical CCVT, after removing couple of repeated zeros and poles found during the simplifications, and is shown in (1).